Aerodynamic and Experimental Analysis of Bio-mimic corrugated dragonfly aerofoil

Md Akhtar KHAN*,[1], Chinmaya PADHY[1]

*Corresponding author
[1]Department of Mechanical Engineering, GITAM Deemed to be University,
Hyderabad -502329, Telangana, India,
khan.akhtar24@gmail.com*, dr.padhy.iitkgp@gmail.com

Abstract: *In this work, experimental and computational approach is used to understand the corrugation attitude of a bio-inspired dragonfly mimicked corrugated airfoil at low Reynolds number varying from 15000 to 75000 to understand the advantages of pleated corrugated airfoil. The CFD analysis is carried out on the 2-dimensional bio-mimetic corrugated 'Pantala flavescens' dragonfly forewing to predict the aerodynamic characteristics of the corrugated dragonfly aerofoil with varying angle of attack from 0° to 8°. The computational analysis of the wing profile is done using the ANSYS-19 ICEM CFD and FLUENT software. For the experimental test, the model is printed in 3-D printer machine and tested in subsonic Wind Tunnel at different speeds and different angle of attacks using a wind tunnel 6-component balance. The computational simulation reveals the exemplary results of the pleated airfoil (corrugated aerofoil) with new design constraints. Finally, the computational result is validated with experimental results.*

Key Words: *ICEM CFD, FLUENT, Pleated airfoil, corrugated wing, Wind Tunnel, Reynolds number*

1. INTRODUCTION

The 'Pantala flavescens' forewing discloses wavy corrugated structure and the corrugation varies along the longitudinal axis rendering aerodynamic characteristics [1]. Dragonfly is unique in nature due to its high maneuverability, low noise and gliding performance that make them most suitable for the MAVs. For the steady level flight, the dragonfly can fly up to an altitude of approximately 100 m intro the air using flapping flight and remains aloft without requiring extra kinetic energy. Thus, this feature is most desirable advantage to implement into MAVs for Power saving capacity [2]. On the other hand, past computational studies [3, 4, 5] relate that the corrugated wing produces higher lift and less drag. In fact, dragonfly wing experiences significant amount of bending and twisting during flight, which will change the aerodynamic as well as the structural response during loading conditions. Usually, insect wings appear to be a flat plate in terms of aerodynamic characteristics. But basically, dragonfly corrugated wings are devised by the wrap of flexible permeable membrane into V-shaped valleys [6]. Numerous studies assert that the kind of mechanism and exemplary smart structure of dragonfly wing can withstand array of loads. The wings have a high stability and are covered with a thin layer of wax being made of chitin and structural proteins (Kesel et al., 1998; Ellington,1984) [7-13, 14, 15]. This work is inspired from the dragonfly wing corrugation located at the radius part of the wing nearly 40% of the total span of the wing from the root.

During gliding flight dragonfly wings are considered as ultra-light aerofoil due to their well-defined cross-sectional corrugation. Most of the researchers [16-21] have investigated the aerodynamic benefits because the flight kinematics of dragonfly insects differs significantly from most of insects.

In the micro air vehicle design, mostly high C_L/C_D ratio, high Power and Low sinking rate is preferred. For high efficiency and long range corrugated wing can perform much better at higher angle of attack (AoA) [21]. The high level of dexterity in wing motion of the dragonfly allows for its excellent maneuverability and superior flight performance than existing designs [22, 23]. In this present work we have considered the pleated aerofoil of subcosta part of forewing of dragonfly and performed the CFD analysis and wind tunnel testing of the pleated aerofoil at different motor RPM and angle of attack to understand the attitude and its benefit over conventional wing structure.

2. GEOMETRY AND CFD ANALYSIS

Fig. 1 shows the two-dimensional model of wavy corrugation profile located at the subcosta of the forewing of dragonfly wing having chord length 110 mm and thickness is 4 mm. The thin pleated aerofoil is considered which is lying at 40% from the root of the wing.
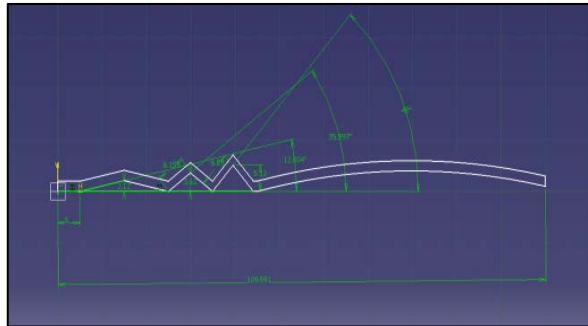

Fig. 1 CATIA V5 model of corrugated aerofoil

The simulation is done in CFD using ANSYS Fluent and ICEM to understand the aerodynamic characteristics of the corrugated pleated aerofoil of given dimension.

The performance is predicted in terms of graphs which emphasizes that the corrugation provides better gliding ratio (C_L/C_D), Maximum Endurance and minimum sinking rate.

The Performance analysis is done for the varying Reynolds number range of Re = 15000 to Re =75000.The boundary conditions are shown in Table 1.

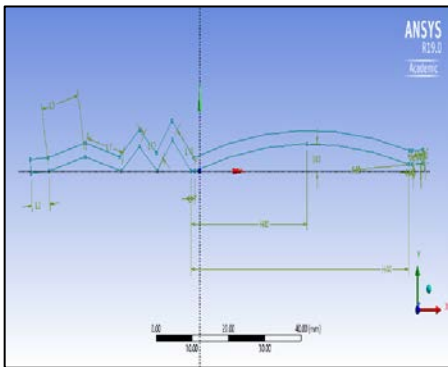Fig. 2 Ansys Geometry model   Fig. 3 Mesh grid at 0°

Table 1. Boundary Conditions

Domain size	910 mm x 610 mm
Dynamic viscosity (μ)	1.7895×10^{-5} Ns/m
Density	1.23 Kg/m^3
Minimum orthogonality	0.511
Inflow velocities (U_∞)	2 m/s, 5m/s and 10m/s
Reynolds number	15000, 37000 and 75000

The model is created in ANSYS geometric model as shown in Fig. 2. After the meshing of the model in ICEM CFD, we exported them to ANSYS 19.0 Fluent and generated a mesh over it and also assigned a domain (i.e. inlet, outlet and walls) as shown in Fig. 3.

3. CFD RESULTS

3.1 CFD Analysis different velocities and angle of attack

- **At 2 m/s Velocity**
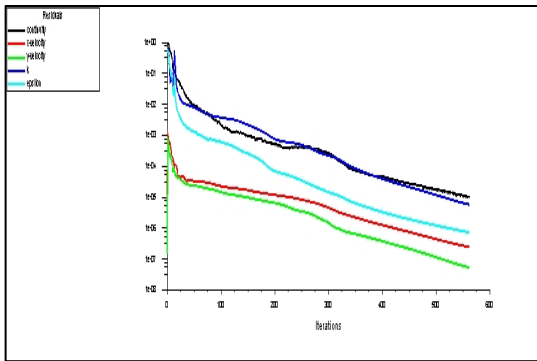
Fig. 4 (a) Convergence at 0° AoA
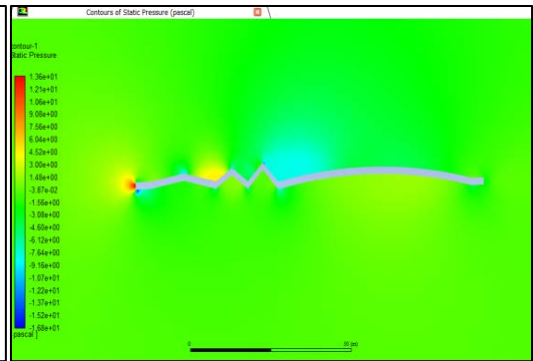
Fig. 4 (b) Pressure contour at 0° AoA
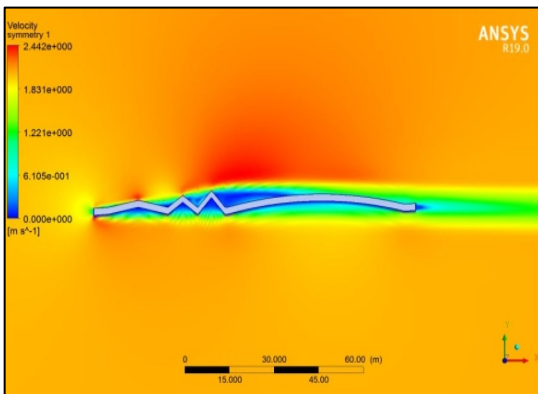
Fig. 4 (c) Velocity contour at 0°
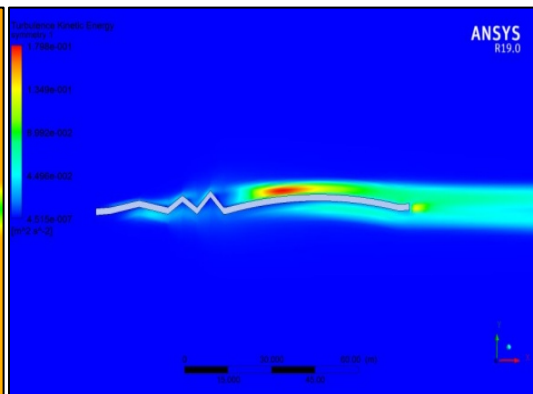
Fig. 4 (d) Turbulence contour at 0°

From Fig. 4(a) and (b) we can observe that at stagnation point the pressure is maximum at the leading edge of the corrugated aerofoil and velocity is zero. After this, there is a uniform pressure distribution over the wing.
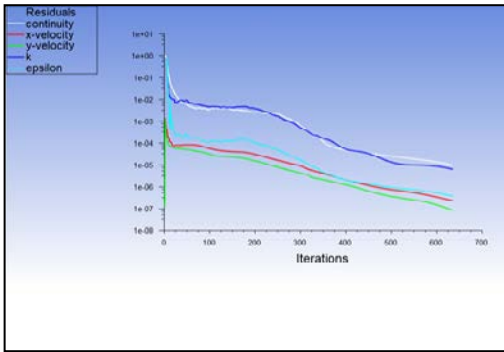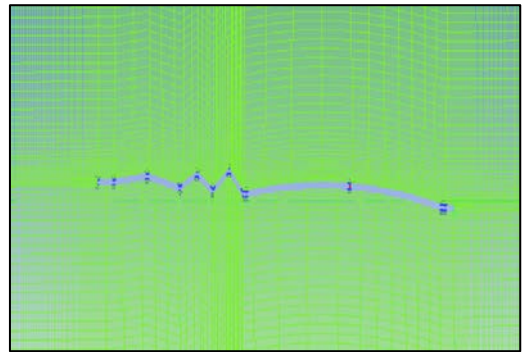
Fig. 4 (e) Convergence at 4° AoA
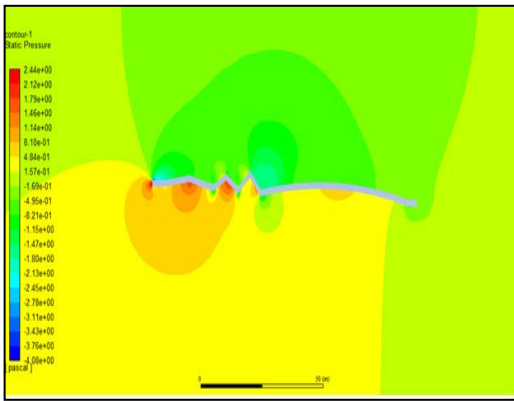

Fig. 4 (f) Mesh grid at 4° AoA

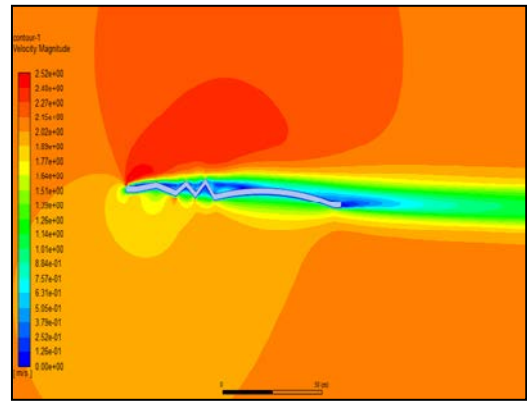Fig. 4 (g) Static pressure contour at 4° AoA
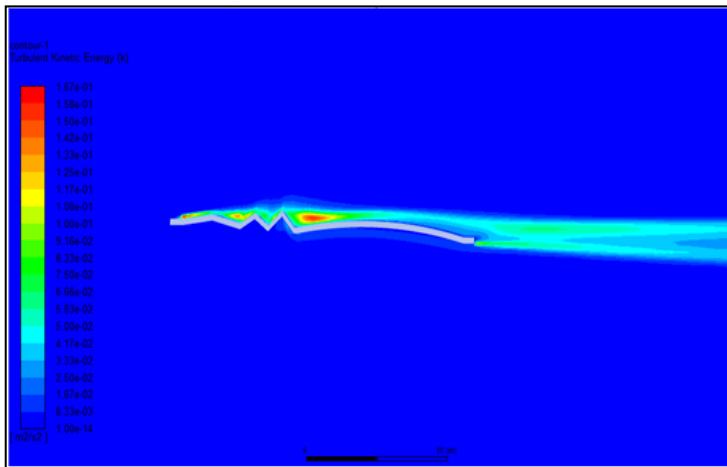

Fig. 4 (h) Velocity contour at 4° AoA

Fig. 4 (i) Turbulence contour at 4° AoA

As shown in Fig. 4(g) as there is linear increment in static Pressure over the pressure side of the corrugated aerofoil, the high pressure difference results in increased lift [22, 23]. The velocity on the upper surface is more at the rear end and the flow left the smooth surface with minimal velocity as shown in Fig. 4(h).

The turbulent eddies flow is formed at the trailing edge, as angle of attack (α) increases as shown in Fig. 4(i).
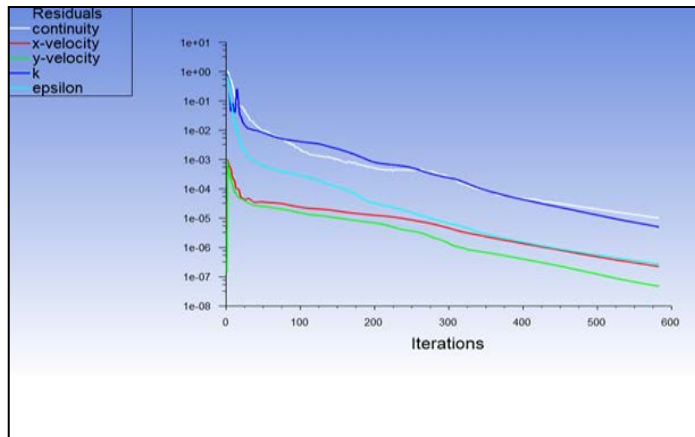
- **At 5 m/s Velocity**
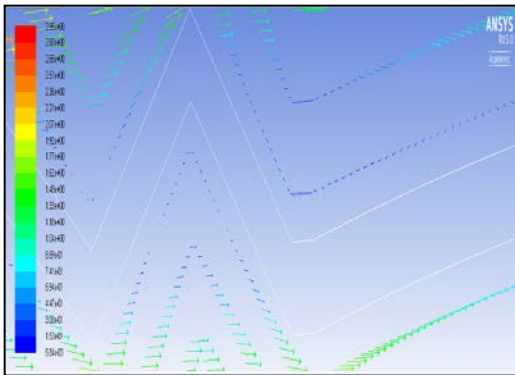

Fig. 5 (a) Convergence at 0° AoA
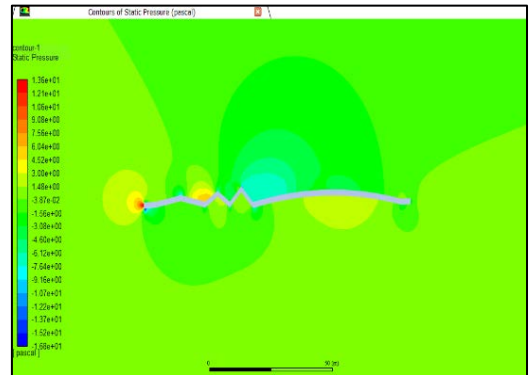

Fig. 5 (b) Flow reversal and reattachment at 0°AoA   Fig. 5 (c) Static pressure contour at 0°AoA
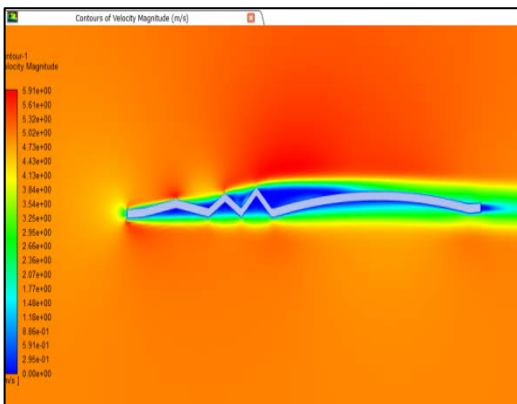

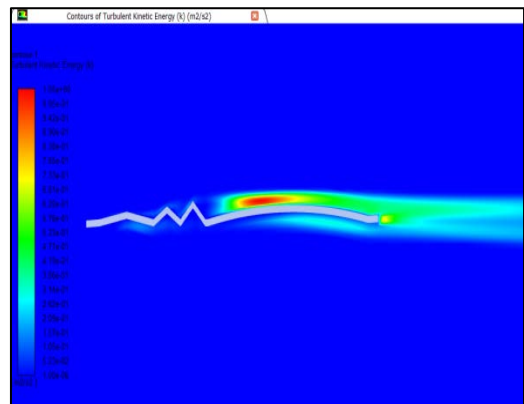Fig. 5 (d) Velocity contour at 0° AoA   Fig. 5 (e) Turbulent contour at 0° AoA
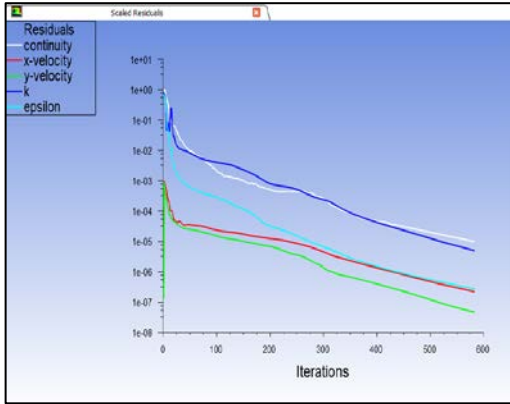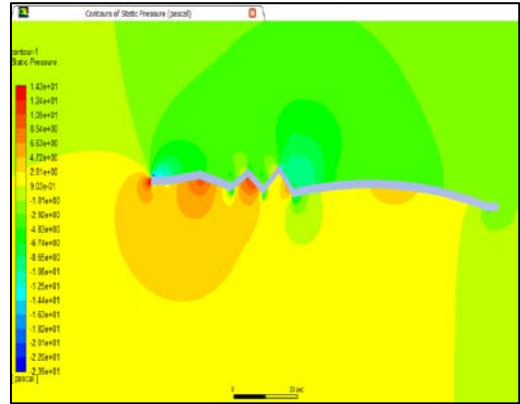
Fig. 5 (f) Convergence at 4° AoA

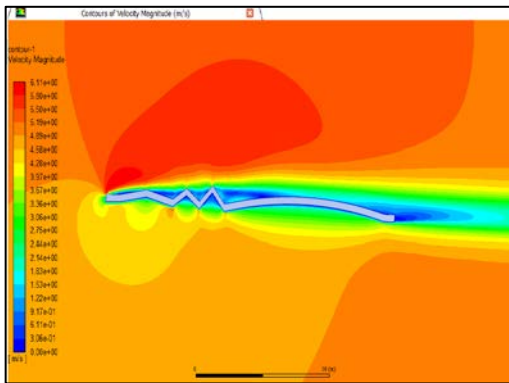Fig. 5(g) Contours of static pressure at 4° AoA
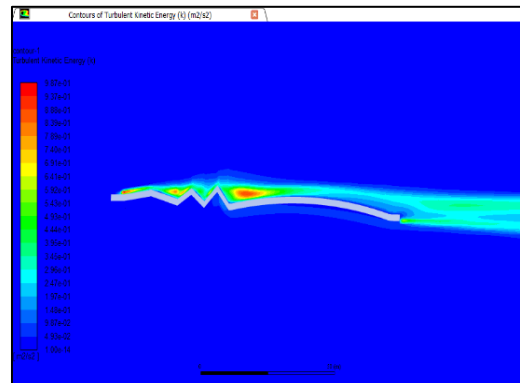

Fig. 5(h) Velocity contours at 4° AoA

Fig. 5(i) Turbulent K.E Contour 4° AoA

As shown in Fig. 5(a) the mesh at 4° AoA is converged. Increasing the angle of attack increases lift and simultaneously increases drag also but for the corrugation wing as the incidence angle increases, the C_L increases resulting in increment of L/D ratio which helps on reducing the eddies and vortices.

The vortices are trapped inside the valley and reattaches to the surface or peak delaying the flow separation.

From Fig. 5(b) we noticed that the flow is trapped inside the third valley of the corrugated aerofoil and delays flow separation where the blue arrows represent reversed flow due to change in pressure gradient and sooner the flow reattaches towards the trailing edges. As the angle of attack angle increases from 0° to 4° the stagnation point start shifting to bottom of the corrugation leading edge and Pressure at the leading edge is maximum where the velocity is zero exhibit in Fig. 5(c) and 5(d). Due to stall the vortices are formed, which results in fall of the lift and the decrease of performances.

The pressure is maximum at the stagnation point which is shifted at the lower edge of the pleated aerofoil, where the maximum pressure is shown in Fig. 5(g).

From Fig. 5(h) we can observe that the velocity on the upper surface is very high which results in less pressure on suction side and high pressure on pressure side and the vortices are trapped inside the valleys as shown in Fig. 5 (i).
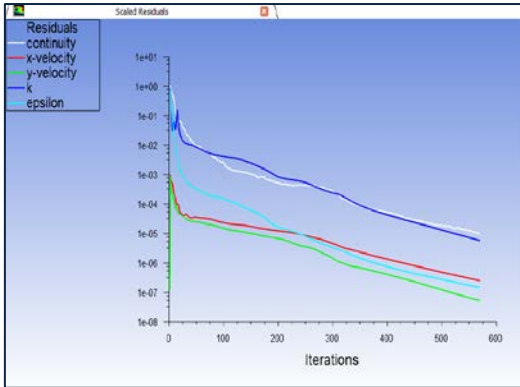
- **At 10 m/s velocity**
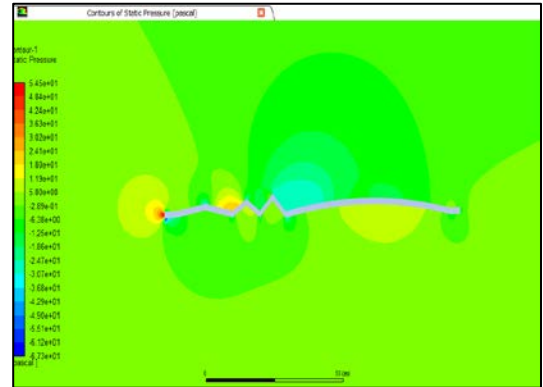

Fig.6 (a) Convergence at 0° AoA

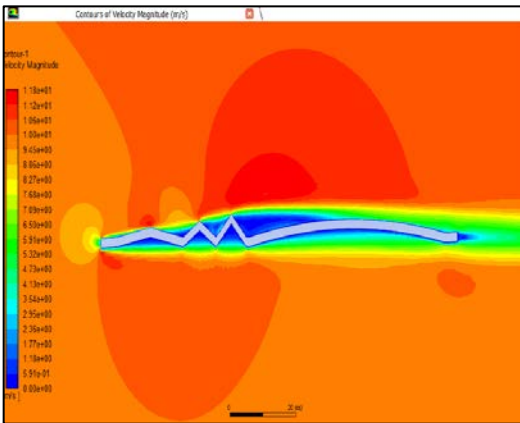Fig.6 (b) Pressure contour 0° AoA

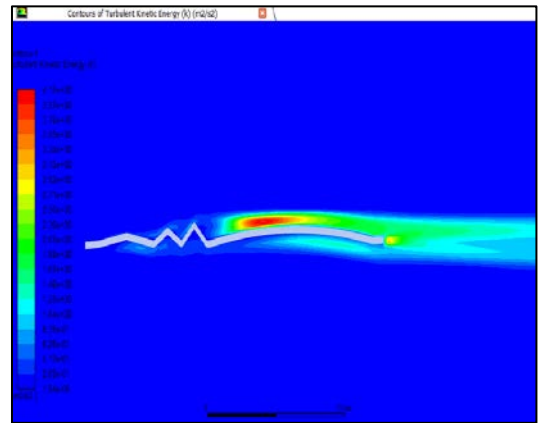Fig. 6 (c) Velocity contour 0°AoA

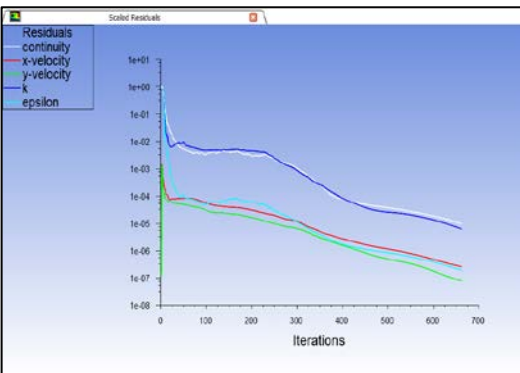
Fig. 6 (d) Turbulent Kinetic Energy Contour 0°AoA

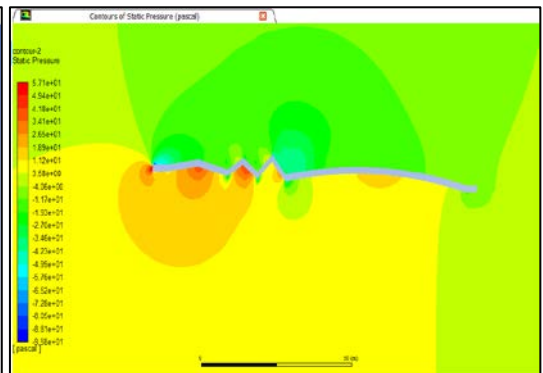Fig. 6 (e) Convergence at 4° AoA

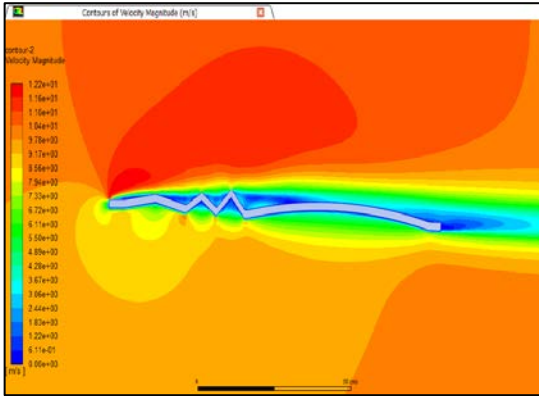Fig. 6 (f) Pressure contour at 4° AoA
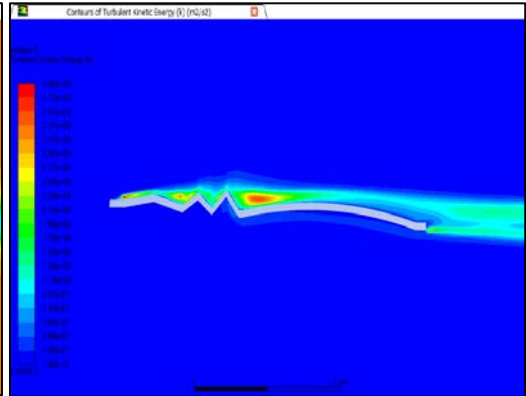
Fig. 6 (g) Velocity contour at 4° AoA　　　　　Fig. 6 (h) Turbulence contour at 4ºAoA

The red dot represents the stagnation point where pressure is higher on the lower part of the wing, which implies velocity is less on the lower surface and there is higher velocity on upper side due to pressure difference results in production of the lift as shown in Fig. 6 (f).

Since high velocity on the upper surface and zero velocity in the valleys indicate flow reversal in the valleys due to pressure difference at the particular location it leads to vortices formation as shown in Fig. 6 (g). The turbulence effect is shown in Fig. 6 (h).

But here the flow is trying to reattaches and the lower surface flow is going to re-energize the upper surface flow delaying the flow separation which gives better L/D ratio.

We know that higher corrugation angle delays the flow separation ensuring better L/D ratio.

The continuous movement of stagnation point from the leading edge to the trailing edge as angle of attack (α) is increased [8, 13].

With increase in angle of attack there is a reverse flow within the valley and reattachment takes place at the trailing edge and flow leaves smoothly over the surface as it is predicted.

The C_L/C_D ratio plays an important role on the range and endurance performance of the MAVs.

If ($\frac{C_L}{C_D}$) ratio is maximum, the range will be maximum. To fly longest distance (maximum range) we should fly the MAVs at speed corresponding to maximum L/D for the corrugated wing [17, 18].
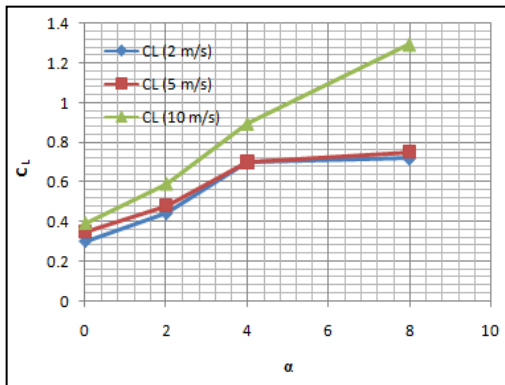

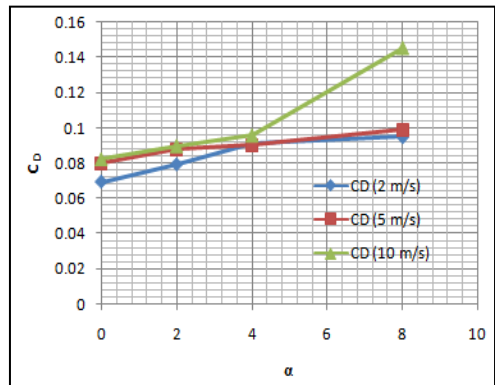Fig. 7 Coefficient of Lift with respect to α [degree]　　Fig. 8 Coefficient of Drag with respect to α [degree]
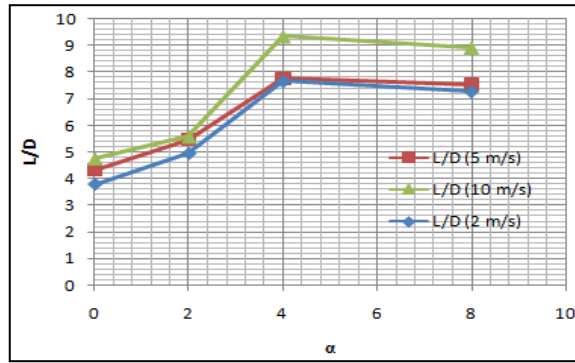
Fig. 9 Lift to Drag ratio with respect to α [degree]

As we can observe from Fig. 7, the coefficient of lift increases with increase in angle of attack as the flow velocity increases in due course of time.

Till 8° AoA, the C_L goes on increasing simultaneously C_D is also higher as shown in Fig. 8. If L/ D ratio is maximum, the range will be maximum, and L/D is maximum at 4 degree and after this it is decreasing slowly at 10m /s, as shown in Fig. 9.

So to fly longest distance (maximum range) the corrugated wing should fly at speed corresponding to maximum L/D.

4. EXPERIMENTAL ANALYSIS

The corrugated wing model is 3D printed using Acrylonitrile Butadiene Styrene(ABS) material having Planform area 110 X 50 mm² and a thickness of 4 mm, as shown in Fig. 10 (a) and 10 (b), but for 2-d experimental analysis we have considered the span as unity (i.e. b=1mm) and only the effect of chord is accounted.

The experimental testing is performed in an open loop wind tunnel test section of size 0.6 m x 0.6m x 2m.

The 6-Component balance is used to get reading of lift forces and drag forces while varying Reynolds number from 15000 to 75000 (as most of the MAVs fly in this range), and at various AoA from 0°(degree) to 8°(degree).

The digital six-component balance is used to do the calculation of aerodynamic forces acting on the wing.
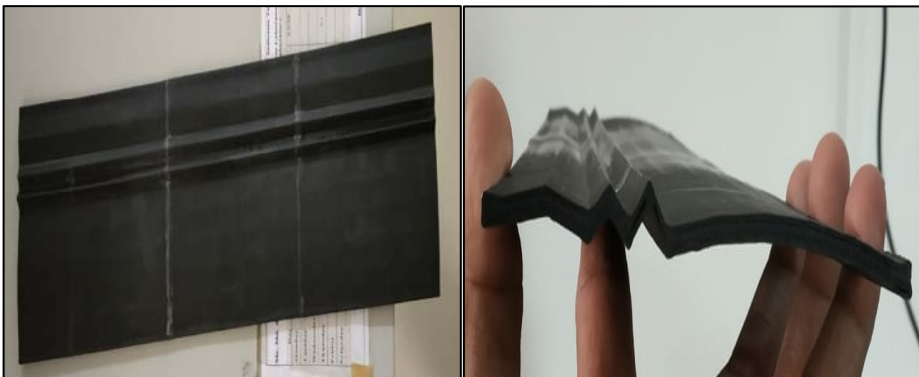
Fig. 10 3-D printed ABS corrugated wing

Fig. 11 Wind Tunnel facility at GITAM University

Fig. 12   Corrugated wing in wind tunnel
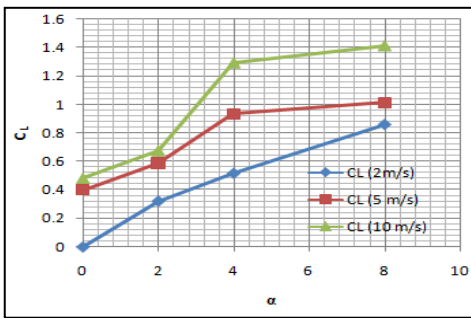
Fig. 13 Coefficient of Lift with respect to α [degree]
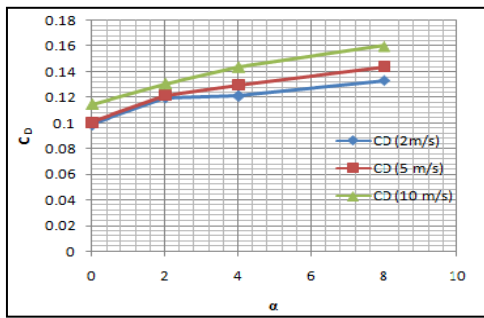
Fig. 14 Coefficient of Drag with respect to α [degree]
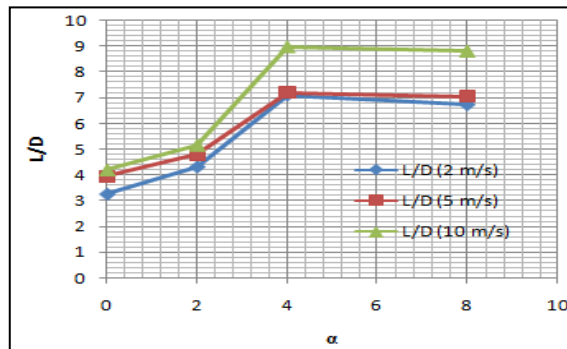
Fig. 15 Lift to Drag ratio with respect to α [degree]

As we can observe, that C_L increases when the incidence angle increases, as depicted in Fig. 13. It is seen that there is drastic increase in lift force as the angle of attack proceeds further and it is maximum at velocity of 10m/s; simultaneously C_D also increases and maintains nearly constant for the range of 4 degrees to 8 degrees, as shown in Fig. 14. The gliding ratio CL/CD is nearly 9, which is maximum at 10m/s, as shown in Fig. 15.

5. VALIDATION OF COMPUTATIONAL AND EXPERIMENTAL RESULTS

The Computational result is validated with the experimental results to understand the accuracy of the flow behaviors for a given Reynolds range of 15000 to 75000, as shown in Table 2, Table 3 and Table 4.

Table 2. Comparison of C_L for Computational and Experimental Results

AoA	Computational Results			Experimental Results		
α	C_L (2m/s)	C_L (5m/s)	C_L (10m/s)	C_L (2 m/s)	C_L (5 m/s)	C_L (10m/s)
0	0.3	0.35	0.39	0.3214	0.3891	0.4821
2	0.442	0.48	0.589	0.4167	0.4849	0.6449
4	0.699	0.701	0.893	0.6593	0.7328	0.92
8	0.72	0.752	1.105	0.7954	0.8926	1.14121

Table 3. Comparison of C_D for Computational and Experimental Results

AOA	Computational Results			Experimental Results		
α	C_D (2m/s)	C_D (5m/s)	C_D (10m/s)	C_D (2m/s)	C_D (5m/s)	C_D (10m/s)
0	0.0692	0.08013	0.08211	0.0987	0.1009	0.1146
2	0.0792	0.08791	0.08961	0.1197	0.1219	0.1307
4	0.09123	0.0903	0.09552	0.1209	0.1298	0.1438
8	0.0948	0.0989	0.1451	0.1329	0.1439	0.1603

Table 4. Comparison of L/D ratio for Computational and Experimental Results

| AOA	Computational Results			Experimental Results		
α	L/D (2m/s)	L/D (5m/s)	L/D (10m/s)	L/D (2m/s)	L/D (5m/s)	L/D (10m/s)
0	3.787	4.3304	4.7509	3.256	3.9554	4.2068
2	4.9473	5.4749	5.5762	4.3166	4.7981	5.1637
4	7.663	7.7674	9.348	7.1075	7.1864	8.9777
8	7.2804	7.5449	8.9255	6.7373	7.0368	8.8091

Fig. 16 Coefficient of lift with respect to α [degree]
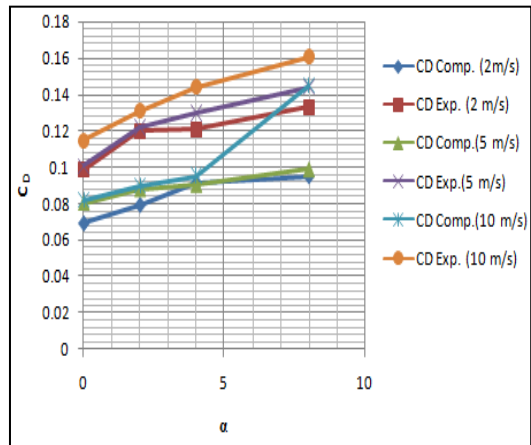
Fig. 17 Coefficient of Drag with respect to α [degree]

Fig. 18 Lift to Drag ratio with respect to α [degree]
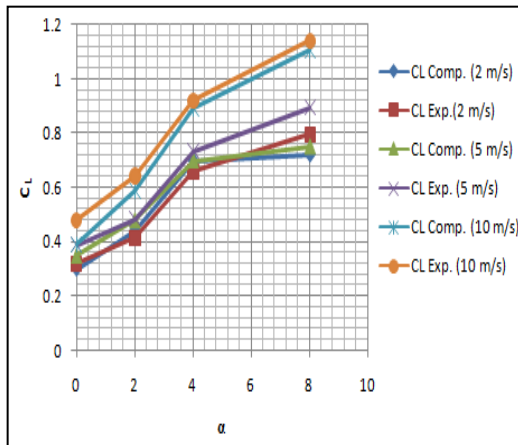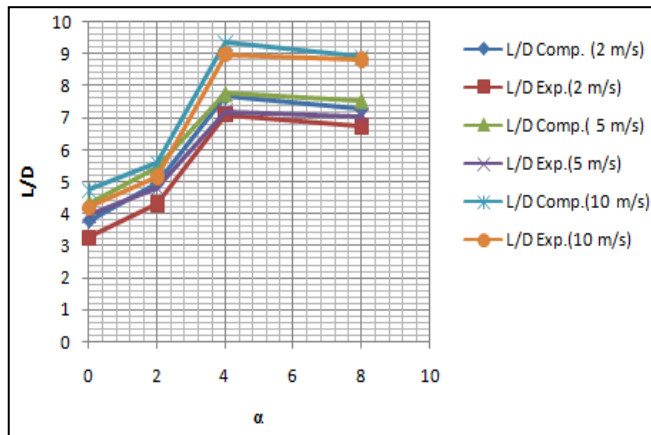
6. CONCLUSIONS

The present work relates to the aerodynamic performance and experimental analysis of 2-d corrugated aerofoil of the dragonfly located at 40% of the forewing near the subcosta part of the forewing. The observation from computational analysis is that the corrugated wing is more suitable for low Reynolds number flyer at lower angle of attack.

The corrugated airfoil acts as tabulators and delays the flow separation and stall. We also observed that the pleated aerofoil is giving better lift to drag ratio and the results are consistent near the radius or subcosta part of the forewing, as being considered.

TheWind Tunnel testing experiment indicates that there is less flow separation and flow reattaches in the valleys, even at lower angle of attack the L/D ratio is higher compared to conventional aerofoil at a particular angle.

The validation tells that the computational and experimental results are really close and comparable.

These results give useful understanding and characterization of rigid flapping wing flight and aid to the design of highly agile micro air vehicle.

ACKNOWLEDGEMENTS

REFERENCES

[1] Y. H. Chen and M. Skote, Study of lift enhancing mechanisms via comparison of two distinct flapping patterns in the dragonfly sympetrum flaveolum, *Physics of Fluids* **27**, 033604, 2015.
[2] D.-E. Levy and A. Seifert, Simplified dragonfly airfoil aerodynamics at Reynolds numbers below 8000, *Physics of fluids*, **21** (7), 071901, 2009.
[3] S. A. Combes, T. L. Daniel, Flexural stiffness in insect wings. II. Spatial distribution and dynamic wing bending, *J. Exp. Biol.,* **206**:2989–2997, 2003.
[4] D. J. S. Newman, R. J. Wotton, An approach to the mechanics of pleating in dragonfly wings, *J.Exp.Biol.*, **125**, 361-372, 1986.
[5] D. J. S. Newman, R. J. Wootton, An approach to the mechanics of pleating in dragonfly wings, *Journal of Experimental Biology*, **125**: 361–372, 1986.

[6] C. J. C. Rees, Aerodynamic properties of an insect wing section and a smooth aerofoil compared, *Nature*, **258**: 141–142, 1975a, DOI: 10.1038/258141a0.

[7] K. Hord, Y. Lian, *Numerical Investigation of the aerodynamic and Structural Characteristics of a corrugated airfoil*, 40th Fluid Dynamics Conference and Exhibit, 2010.

[8] Y. H. Chen and M. Skotes, Gliding Performance of 3D corrugated dragonfly wing with spanwise variation, *Journals of Fluid and structures*, 2016.

[9] J. Murphy and H. Hui, An Experimental investigation on a Bio-inspired corrugated airfoil, *47th AIAA aerospace science meeting including the new horizons Forum and Aerospace Exposition*, 2009.

[10] A. B. Kesel, Aerodynamic characteristics of dragonfly wing sections compared with technical aerofoils, *J. Exp. Biology*, **203**: 3125-3135, 2000.

[11] H. Hui, T. Masatoshi, Bioinspired corrugated airfoil at low Reynolds number, *Journal of Aircraft*, 2008.

[12] B. S. Lazos, Biologically Inspired Fixed-wing configuration studies, *Journal of Aircraft*, 2005.

[13] A. Vargas, A computational study of the aerodynamic performance of adragonfly wing section in gliding flight, *Bio-inspiration and Biomimetics*, 2008.

[14] K. Hord, Y. Lian, Numerical Investigation of the aerodynamic and structural characteristics of a corrugated airfoil, *40th Fluid Dynamics Conference and Exhibit*, 2010.

[15] H. Liu, C. P. Ellington, K. Kawachi, C. Van Den Berg and A. P. Willmott, A computational fluid dynamic study of hawkmoth hovering, *J. Exp. Biol.*,**201**, 461-477, 1998.

[16] R. J. Wootton, R. C. Herbert, P. G. Young, K. E. Evans, Approaches to the structural modeling of insect wings, *Phil Trans R Soc B*, **358**:1577–1587, 2003.

[17] B. S. Lazos, Biologically Inspired Fixed-Wing Configuration Studies, *Journal of Aircraft*, Vol. **42**, No.5, September-October, 2005.

[18] M. Tamai, Z. Wang, G. Rajagopalan, H. Hui and G. He, Aerodynamic Performance of a corrugated dragonfly airfoil compared with smooth airfoils at Low Reynolds number, *45th AIAA Aerospace Science meeting and Exhibit*, 2007.

[19] T. J. Flint, M. C. Jermy, T. H. New, W. H. Ho, Computational study of bio-inspired corrugated airfoil, I. J. of heat and fluid flow, int. *Journal of Heat and Fluid flow*, **65**: 328-341, doi.2016.12.009,2017.

[20] M. A. Khan, C. Padhy, H. M. Nandis, K. Rita, Computational Analysis of Bio-Inspired Corrugated Airfoil with Varying Corrugation Angle, *Journal of Aeronautics & Aerospace Engineering*, **7**:208, doi-10.4172/2168-9792, 2018.

[21] A. Khan, C. Padhy, Aerodynamic and structural analysis of bio-mimetic corrugated wing, *Fluid mechanics research international journal*, vol. **3**, doi: 10.513.03.00053, 2019.

[22] K. Machida, T. Oikawa, J. Shimanuki, The effect of the costal vein configuration of the wings of a dragonfly, *Key Eng. Mater.*, vol. **326-328**: 819-822, 2006.

[23] T. A. Swanson, An experimental and numerical investigation of flapping and plunging wings, Phd thesis, Department of Mechanical and Aerospace Engineering, *Missouri university of science and technology, Rolla, Missouri*, 2009.